

DOPPLER TOMOGRAPHY OF CATAclysmic VARIABLES: WHAT CAN WE DO WITH THE GTC?

J. Echevarría,¹ R. Costero,¹ L. Pineda,¹ G. Tovmassian,² S. Zharikov,² and R. Michel²

RESUMEN

Se está llevando a cabo un proyecto a largo plazo para observar una muestra grande de variables cataclísmicas con espectroscopía de alta resolución ($R \sim 20000$) con el espectrógrafo echelle en el telescopio de 2.1 m del Observatorio Astronómico Nacional en San Pedro Mártir, Baja California, México. Series de tiempo de un número de objetos, cubriendo varios períodos orbitales se han usado para crear mapas de los discos de acreción usando la técnica de Tomografía Doppler. Presentamos aquí resultados preliminares y discutimos como podríamos mejorar este tipo de observaciones con el GTC y un espectrógrafo de alta resolución.

ABSTRACT

We are conducting a long-term project to observe a wide sample of cataclysmic variables with high resolution spectroscopy ($R \sim 20000$) using the echelle spectrograph at the 2.1 m telescope at the Observatorio Astronómico Nacional at San Pedro Mártir Observatory in Baja California, Mexico. Time series of a number of objects covering several orbital periods have been used to map their accretion disks using the Doppler tomography technique. We present preliminary results and discuss how can we take advantage of the GTC high resolution spectrograph to improve these kinds of observations.

Key Words: BINARIES: CLOSE — STARS: INDIVIDUAL: EY CYG, AE AQR, 1WGA J1958.2+3232, SS AUR, V751 CYG, WZ SGE — STARS: NOVAE, CATAclysmic VARIABLES

1. INTRODUCTION

The project goal in this research is to map the accretion disks in cataclysmic variables in order to to examine the accretion mechanisms in these interactive stars. We are using a technique developed by (Marsh & Horne 1988). This method, called Doppler tomography, maps the emission profiles of lines arising from the accretion disk as a function of the orbital phase and reconstructs such a disk into a velocity space map. Although it would be ideal to reconstruct the accretion disk in space coordinates taking a second step from the velocity space map (i.e., to produce a genuine picture of a disk), this would require very high quality spectral profiles taken every few seconds and a with a good orbital period coverage. In the absence of such capabilities, (Marsh & Horne 1988) and (Spruit 1994) have developed maximum-entropy (ME)-based Doppler algorithms to reconstruct the accretion disks in velocity space. This in a half-way step to a true disk; translating the velocity and phase of specific regions of the disk (which produce an S-wave during an orbital cycle) by summing the flux along the track to corresponding *differential* regions in the emission line in proportion to the total flux.

In this contribution, we present preliminary results of Doppler tomography obtained mainly with the echelle spectrograph at our 2.1 m telescope and discuss how the GTC and a high resolution spectrograph could improve our results and contribute to the ultimate goal of reconstructing a real accretion disk.

2. SPECTRAL OBSERVATIONS

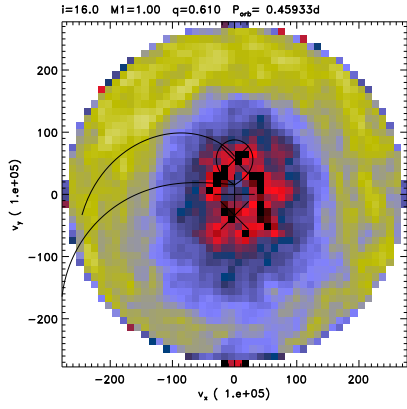
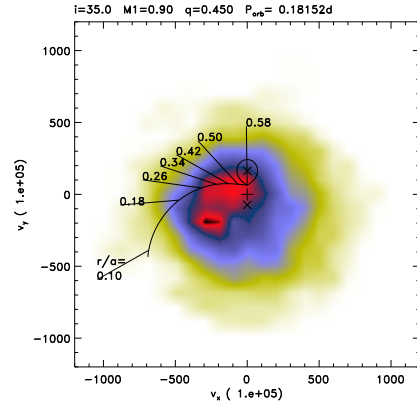
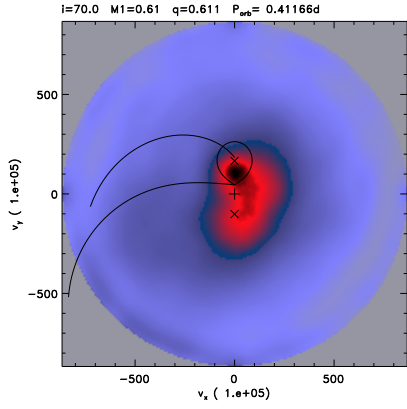
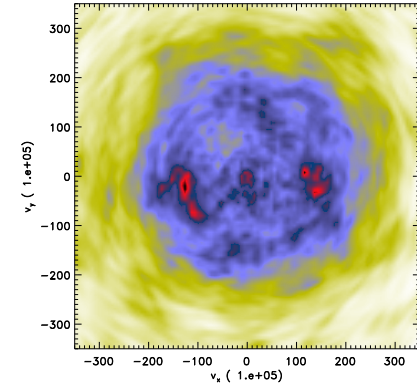
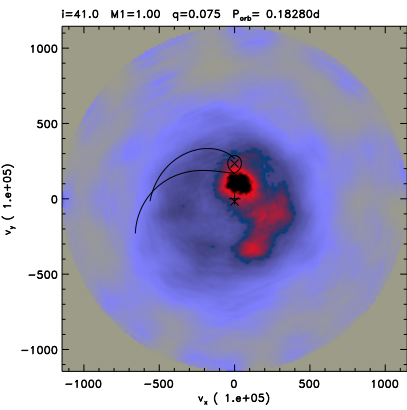
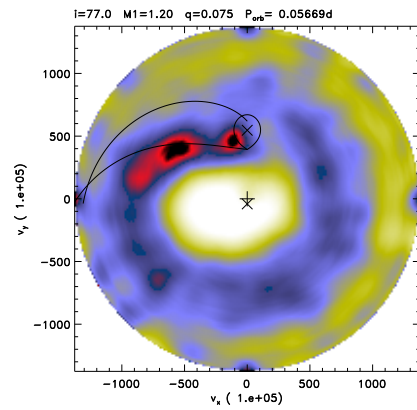
Observations of five of the six objects shown in Table 1 were obtained with the Echelle Spectrograph attached to the 2.1 m telescope at the Observatorio Astronómico Nacional on different observing runs from 1993 to 2002. The coverage is from 3700 to 7000 Å. We used several CCDs with pixel sizes ranging from 15 to 24 μm and a spectral resolution from 13 to 18 km s^{-1} . For comparison, we have included an already-published object, 1WGA J1958.2+3232, which was observed at lower resolution with the Boller & Chivens Spectrograph (Zharikov et al. 2001). The full and detailed results of the other five objects will be published elsewhere.

3. THE DOPPLER TOMOGRAPHY OF A CATAclysmic VARIABLE SAMPLE

We present in Figures 1–6 Doppler tomography of six objects in our sample. They are plotted according to their orbital periods, with the largest at

¹Ciudad Universitaria, México, D.F., México.

²Unidad Ensenada, Baja California, México.

Fig. 1. H_α Doppler map of EY Cyg.Fig. 4. H_β Doppler map of 1WGA J1958.Fig. 2. H_β Doppler map of AE Aqr.Fig. 5. H_α Doppler map of V751 Cyg.Fig. 3. H_α Doppler map of SS Aur.Fig. 6. H_α Doppler map of WZ Sge.

the top left and the shortest at the bottom right. In the resulting tomograms the secondary, set at orbital phase 0.0 for inferior conjunction, is at the top, while the primary star is below, near zero velocity. In most cases we have overlapped the Roche lobe of the secondary star, the stream path, and Kepler velocity along the stream (solid lines). The crosses represent the position of the white dwarf, the plus sign, the center of mass; the stream radius and azimuth relative to the primary are annotated. These overlaps are based on assumed parameters of the binary, which are shown at the top of most figures (except for V751 Cyg). The basic parameters are: i , the inclination of the orbital plane of the binary with respect of the observer; M_1 , the mass of the primary star; $q = M_2/M_1$; the mass ratio; and P_{orb} , the orbital period. A full disk should result in an broad annulus, an inside-out disk, centered on the white dwarf, with minimum velocities in a circle with radius somewhat outside the secondary Roche lobe and maximum velocities with a cut-off at the corresponding radius where the material reaches the primary star at maximum Keplerian velocities. A full disk is not present in all objects. We found evidence of such a disk only in EY Cyg and WZ Sge (taken on 2001 August 29, during superoutburst) and probably in V751 Cyg, although we believe we need better map resolution for this object. In AE Aqr and SS Aur, we find evidence of a hot-spot associated with the secondary star and stream material around the primary star. This is common in intermediate polars, where the magnetic field of the white dwarf inhibits the presence of a full disk. We have included an H_β map of 1WGA J1958.2+3232, taken with the B&Ch spectrograph from (Zharikov et al. 2001). This is an example of an intermediate polar where only the stream and the hot-spot of the accretion disk are clearly seen. The Doppler map in this case was constructed with spectra at a resolution of $R \sim 1800$, while the echelle H_β and H_α maps have been obtained from spectra at a resolution of $17000 \leq R \leq 20000$. As the main purpose of this contribution is to examine the scientific possibilities of the GTC, in the next section we discuss the possible advantages of having a very high resolution spectrograph on the new telescope.

4. WHAT CAN WE IMPROVE WITH THE GTC?

In order to have a good quality Doppler tomogram we need to have comparable wavelength and phase bins with a good signal-to-noise ratio and an accurate timing. For low resolution spectra this is

not a problem. As (Spruit 2001) has pointed out, if the velocity area of interest has a velocity v and your wavelength resolution is $R = \lambda/\Delta\lambda$, then the optimal phase resolution in units of orbital period is:

$$\Delta\Phi = \frac{c}{v} \frac{1}{2\pi R}. \quad (1)$$

In the last two columns of Table 1, we show the observed phase coverage derived from the tabulated orbital period and exposure time,

$$\Delta\Phi(\text{obs}) = P_{\text{orb}}(s)/t(s), \quad (2)$$

and the corresponding maximum velocity v_{max} ,

$$v_{\text{max}} = \frac{c}{\Delta\Phi(\text{obs})} \frac{1}{2\pi R}, \quad (3)$$

which results from combining equations (1) and (2). Only in the cases of EY Cyg, V751 Cyg and 1WGA J1958.2+3232 can we achieve enough velocity resolution because, in all three cases, the emission lines show very low radial velocity profiles. The observed radial velocities do not exceed 200 km s^{-1} in EY Cyg and V751 Cyg, whereas in 1WGA J1958.2+3232 the observed spectral resolution is only 1800. Also, the material does not exceed 600 km s^{-1} . In the cases of AE Aqr and SS Aur, we have reduced the velocity bins by a factor of 0.7 to construct the Doppler maps because in the ME map algorithm, memory usage becomes critical for large maps. Only velocities below 150 km s^{-1} are well resolved in these two maps. Finally, although the Doppler tomogram of WZ Sge clearly shows a full (although non-symmetric) disk, and velocities above 1000 km s^{-1} seem well resolved, we have co-added several orbital cycles to reduce the nominal exposure time. The object was observed in decline from superoutburst during the fourth echo (Patterson et al 2002). Full results of the WZ Sge campaign are in preparation (Echevarría et al. 2002a; Echevarría et al. 2002b; Costero et al. 2002).

For a good quality map we need a high signal-to-noise ratio S/N . In spectra, S/N (in e^-/pixel in the echelle dispersion direction) is given by

$$S/N = \left(948 \times 10^{-V/2.5} \epsilon A \Delta x Q_{\text{eff}} t \right)^{1/2} \quad (4)$$

(Levine & Chakrabarty 1994), where ϵ is the combined transmission of the atmosphere, telescope, and spectrograph; A is the telescope collecting area; Δx is the CCD pixel resolution in $\text{\AA}/\text{pixel}$; Q_{eff} is the Q.E. of the CCD in e^-/photon , and t is the integration time in seconds. This relation is strictly valid

TABLE 1
OBSERVED OBJECTS AND PARAMETERS

Name	Orbital period (day)	Magnitude (V)	S/N^a (λ 4861 Å)	Exp. time (s)	Phase bin $\Delta\Phi(\text{obs})$	v_{max} (km s $^{-1}$)
EY Cyg	0.4594	15.5	11.4	600	0.0151	158
AE Aqr	0.4116	11.8	62.6	600	0.0169	141
SS Aur	0.1837	14.5	12.7	300	0.0189	126
1WGA J1958.2+3232	0.1813	15.0	29.1	700	0.0447	593
V751 Cyg	0.1449	14.5	18.1	600	0.0479	49
WZ Sge	0.0566	11.5 ^b	39.4	180	0.0368	65

^aThe signal to noise ratio is calculated in Section 4.

^bThe object was on decline from superoutburst; $V(\text{min}) = 14.9$.

at the monochromatic flux at $\lambda 5556$ Å, but can be used as a rough estimate at other wavelengths.

In our best case with the echelle and the 2.1 m telescope we have: $A = 31416$ cm 2 , $R = 20000$, $\lambda = 4,861$, $\Delta x = 0.24$ Å pixel $^{-1}$, $\epsilon = 0.06$ (echelle + telescope), and $Q_{\text{eff}} = 0.80$ we have:

$$S/N = 586 \times t^{1/2} \left(10^{-V/2.5}\right)^{1/2}. \quad (5)$$

In Table 1, we have applied (5) from the actual integration times and V magnitudes; the faint objects have very poor S/N values. Variations in the map fluxes lower than these limits should be discarded.

With the GTC, assuming the same instrumental configuration and efficiency responses as for the echelle, the S/N will simply scale with the new collector area, $A = 785400$ cm 2 :

$$S/N = 4740 \times t^{1/2} \left(10^{-V/2.5}\right)^{1/2}. \quad (6)$$

For very large orbital period systems like EY Cyg, we can reach $S/N = 57$ for the same exposure time without losing orbital resolution. In the extreme case of WZ Sge in quiescence at $V = 14.9$ (Costero et al. 2002), we can obtain, for $\Delta\Phi(\text{obs}) = 0.01$ (i.e., $t = 49$ s), $S/N = 35$. In this case we shall truly reach optimal velocity time and spectral resolution for $v_{\text{max}} = 240$ km s $^{-1}$. To reach a velocity of about 1000 km s $^{-1}$ for the same R we need in general $\Delta\Phi(\text{obs}) = 0.0024$. For WZ Sge at minimum, this implies $t = 12$ s, which will give $S/N = 17$. Thus even with the GTC we shall not reach this limit unless we reduce the spectral resolution.

5. CONCLUSIONS

It is evident from the discussion above that a high dispersion spectrograph ($R \sim 20000$) on the GTC would be desirable for our research. Many accretion disks in cataclysmic variables could be properly resolved, even if we keep low efficiency values in our instrument. Modern optics, of course, could help to greatly improve efficiency losses, especially those of the echelle and echellete gratings, which transmit only 40% of the light each. Detector quantum efficiencies are now reaching near 100%, so it might be possible to improve the numbers derived above.

REFERENCES

- Costero, R., Echevarría, J., Michel, R., Zharikov, S. $\frac{1}{2}$ V., Tovmassian, G. H., Arellano-Ferro, A., & Richer, M. 2002, in preparation
- Echevarría, J., Costero, R., Tovmassian, G. H., Zharikov, S. V., Michel, R., Richer, M., & Arellano-Ferro, A. 2002, in Classical Nova Explosions (New York: AIP), in press
- Echevarría, J., Costero, R., Michel, R., Tovmassian, G. H., Zharikov, S. V., Richer, M. & Arellano-Ferro, A. 2002, ApJL, submitted
- Levine, S., & Chakrabarty, D. 1994, Reporte Técnico MU-94-04, Instituto de Astronomía, UNAM
- Marsh, T. R., & Horne, K. 1988, MNRAS, 235, 286
- Patterson, J. et al., 2002, PASP, 114, 721
- Spruit, H. C. 1994, A&A, 289, 441
- Spruit, H. C. 2001, Dopmap: Doppler mapping of disks in binaries, Version 2.3.1, Documentation, 22 Jan 2001
- Zharikov, S. V., Tovmassian, G. H., Echevarría, J., & Cárdenas, A. A. 2001, A&A, 366, 834

- J. Echevarría, R. Costero, and L. Pineda: Instituto de Astronomía, UNAM, Apartado Postal 70-264, 04510 México, D.F., Mexico (jer, costero, pineda@astroscu.unam.mx)
- G. Tovmassian, S. Zharikov, and R. Michel: Instituto de Astronomía, UNAM, Apartado Postal 877, 22800 Ensenada, Baja California, Mexico (gag, sergey, rmm@astrosen.unam.mx)